Journal of Advanced Ceramics
2014, 3(2): 137–146
DOI: 10.1007/s40145-014-0104-2

ISSN 2226-4108
CN 10-1154/TQ

Research Article

Mechanical and dielectric behaviors of perovskite (Ba,Sr)TiO_3 borosilicate glass ceramics

Avadhesh Kumar YADAV[a,*], C. R. GAUTAM[a], Abhinay MISHRA[b]

[a]*Department of Physics University of Lucknow*, *Lucknow-226007*, *India*
[b]*School of Materials Science and Technology*, *Indian Institute of Technology*, *Banaras Hindu University*, *Varanasi-221005*, *India*

Received: February 18, 2014; Revised: March 14, 2014; Accepted: March 18, 2014

Abstract: Perovskite (Ba,Sr)TiO_3 glass ceramics were crystallized in the presence of La_2O_3 for glass ceramic system $[(Ba_{1-x}Sr_x)TiO_3]$–$[2SiO_2$–$B_2O_3]$–$[K_2O]$–$[La_2O_3]$ ($x = 0.0$ and 0.4). The formation of major crystalline phase of $BaTiO_3$ along with secondary phase of $Ba_2TiSi_2O_8$ was confirmed by X-ray diffraction (XRD) studies. Major crystalline phase was clearly seen in the micrographs of (Ba,Sr)TiO_3 borosilicate glass ceramic samples. The prepared glass ceramic samples showed very high values of toughness and elastic modulus. Barium strontium titanate (BST) glass ceramics are used in barrier layer capacitors for storage of high energy due to their very high dielectric constant and low dielectric loss.

Keywords: (Ba,Sr)TiO_3; X-ray diffraction (XRD); scanning electron microscopy (SEM); elastic modulus; dielectric constant

1 Introduction

Glass ceramics are polycrystalline materials formed by controlled crystallization of glasses, and they possess very high mechanical strength [1]. The mechanical strength of glass ceramics depends on structural composition and processing variables, and it has complex inter-relationship with microstructure [2,3]. The size, shape, natural wetting and presence or absence of internal cracks are also affecting the microhardness of glass ceramics [4]. Gomma *et al.* [5] reported the electrical and mechanical properties of alkali $BaTiO_3$ alumino–borosilicate glass ceramics containing Sr or Mg. In this glass ceramic system, it was seen that microhardness depends on SrO/BaO or MgO/Al_2O_3. The measurement of mechanical properties such as hardness and elastic modulus of sintered $BaTiO_3$ ceramic shows the grain size dependence of densification, and it was found that the microhardness increases with decrease in grain size [6]. The carbon nanotube in the glass matrix enhances the toughness of composite materials.

The variation in electric behavior is due to a sequence of phase transitions and the space charge polarization between glass matrix, crystalline phases and inter grain boundary. At high temperature, $BaTiO_3$ is paraelectric with cubic structure. On cooling, this material undergoes successive structural phase transitions from cubic, tetragonal, orthorhombic and rhombohedral [7]. Such glass ceramics are mainly used in high energy storage device such as barrier layer capacitors. When some of Ba^{2+} ions are replaced by Sr^{2+} ions, electrical properties are extensively changed due to space charge polarization. BST (barium strontium titanate) glass ceramics have perovskite

* Corresponding author.
E-mail: yadav.av11@gmail.com

structure and show ferroelectric behavior. Divya *et al.* [8,9] have investigated the crystallization and dielectric properties of BST borosilicate glass ceramics. This group has also reported dielectric behavior of BST with addition of bariumaluminosilicate. They found that the dielectric constant is 10 000 in bariumaluminosilicate system, but the replacement of aluminosilicate with borosilicate enhances the dielectric constant up to 12 000. BST glass ceramics in Al_2O_3 addition make the dielectric constant of 1000 and breakdown strength of 800 kV/cm [10,11]. The replacement of AlF_3 by Ga_2O_3 in glass ceramic system $60(Ba_{0.7}Sr_{0.3})TiO_3$–$25SiO_2$–$15AlF_3$ have enhanced the crystallization, while Bi_2O_3 retards the crystallization. $Ba_{0.4}Sr_{0.6}TiO_3$ in the presence of 5 vol% BaO–SiO_2–B_2O_3 glass has the highest energy density of 0.89 J/cm^3, which is 2.4 times higher than that of pure $Ba_{0.4}Sr_{0.6}TiO_3$ (0.37 J/cm^3). The improvement of energy density could be mainly due to the increase of the breakdown strength and the decrease of the remnant polarization. Glass ceramics barium/lead based sodium niobates and barium titanate based silicates are investigated, whose dielectric constant are ranging from 20 to 700 [12–14]. The breakdown strength of 1400 kV/cm and the energy storage density of 4.0 J/cm^3 show strontium barium niobate based glass ceramics as strong candidate for high energy density storage capacitors for portable or pulsed power applications, and the breakdown strength increases with crystallization temperature [15]. The increase of Sr/Ba ratio supports the formation of uniform dense and fine-grained structure in glass ceramics, suppresses the crystallization of strontium barium niobate based borate glass, and leads to raised breakdown strength but decreased dielectric constant [16]. Dielectric properties of BST glass ceramics depend upon crystallization, composition of glass ceramic system and doping elements. Recently, our group reported the crystallization and dielectric behavior of BST borosilicate glass ceramics with addition of La_2O_3. La_2O_3 in BST glass ceramics enhances the crystallization and it acts as nucleating agent for crystallization [17,18]. In our previous reported works, the dielectric constant was found to be about 350. Mechanical behavior of BST borosilicate glass ceramics was not reported so far in literature as per best of our knowledge. So, we are trying for enhancing the dielectric constant and mechanical strength of glass ceramics in system $[(Ba_{1-x}Sr_x)TiO_3]$–$[2SiO_2$–$B_2O_3]$–$[K_2O]$–$[La_2O_3]$ ($x = 0.0$ and 0.4).

2 Experimental

2.1 Glass and glass ceramic sample preparation

High purity inorganic ingradients $BaCO_3$ (99%), $SrCO_3$ (99%), TiO_2 (99%), SiO_2 (99.5%), H_3BO_3 (99.8%), K_2CO_3 (99.9%) and La_2O_3 (99.9%) of HiMedia Laboratories Pvt. Limited, India were used for the preparation of glass samples in composition system $[(Ba_{1-x}Sr_x)TiO_3]$–$[2SiO_2$–$B_2O_3]$–$[K_2O]$–$[La_2O_3]$ ($x = 0.0$ and 0.4). The appropriate amounts of these ingredients were mixed in a mortar with pestle in acetone medium. Well mixed and dried powder of raw materials was melted in platinum crucible with high temperature SiC programmable electric furnace at 1200 ℃. Finally, well melted ingredients were poured into an aluminum mould and pressed by a thick aluminum plate. Then, the quenched glass samples were immediately transferred into a preheated programmable muffle furnace for annealing at 450 ℃ for 3 h. Now, the prepared glass samples were grinded in mortar with pestle to form the fine powder, and this glass powder was calcined at 600 ℃ for 3 h with a heating rate of 10 ℃/min. The calcined powder was again grinded using 2.5% of polyvinyl alcohol (PVA) as binder, and pellets (1 cm in diameter) of this powder were formed at load of 10 ton by BEST hydraulic press machine (New Delhi). These pellets were sintered with the heating rate of 5 ℃/min at 850 ℃ for 3 h and 6 h, respectively. Nomenclature of these glass samples was described as: first three alphabets BST denote barium strontium titanate, 5K denotes 5% of K_2O, 1L means 1 mol% of La_2O_3, numeric digit is the fractional content of Sr, T and S denote the sintering time of 3 h and 6 h respectively, and 850 means the sintering temperature (e.g., BST5K1L0.4T850).

2.2 X-ray diffraction

X-ray diffraction (XRD) data of powdered glass ceramic samples was recorded by a Rigaku Miniflex-II X-ray Diffractometer using Cu Kα radiation with step size of 0.02°. XRD patterns of these glass ceramic samples were compared with standard JCPDS files for different constituting phases. The particle size was calculated by Debye–Scherer (DS) method and Williamson and Hall (WH) plots.

2.3 Scanning electron microscopy

Scanning electron microscopy (SEM) is one of the most versatile instruments available for the examination and analysis of the microstructural morphology of solid objects. The glass ceramic samples were polished by using SiC powder of 100 mesh, 600 mesh and 800 mesh to attain the smooth surfaces. These smooth glass ceramic samples were further polished by emery paper of different grades of 1/0, 2/0, 3/0 and 4/0, and the final polishing was done on a blazer cloth using diamond paste (1 μm and 6 μm) with Hifin fluid "OS". Glass ceramic samples were polished and etched using a solution of 30%HNO_3 + 20%HF. Au–Pd coating was done by sputtering method (Poraton Sc-7640 Sputter) on the etched surface of various glass ceramic samples for SEM. SEM images were recorded for surface morphological studies of crystalline phases (voltage of 15 kV and magnification of 5000× by using Model LEO 430 Cambridge Instruments Ltd., UK).

2.4 Density measurements

The geometrical density of green pellets and sintered glass ceramic pellets was measured by using formula of mass unit volume. The geometrical density of these samples has been listed in Table 1.

2.5 Mechanical measurements

Mechanical characterizations were carried out in a universal testing machine (Instron 3639) in compression mode of cylindrical glass ceramic sample having dimensions of 1 cm in diameter and 2.5 cm in length. The toughness of BST borosilicate glass ceramic samples was measured as area under stress–strain curve within limit of initial point to elastic limit point.

2.6 Dielectric measurements

For dielectric measurements of glass ceramic samples, the both surfaces of these samples were made smooth and electroded by applying the silver paint (Code No. 1337-A, Elteck Corporation, India). The electroded samples were cured at 600 ℃ for 5 min. The capacitance C and dissipation factor tanδ were measured at frequencies of 20 Hz, 100 Hz, 1 kHz, 10 kHz and 100 kHz in equal intervals of temperature during heating in the range of room temperature to 150 ℃ by Wayne Kerr 6500 P (high frequency LCR meter, frequency: 20 Hz–5 MHz). The samples were heated in the heating chamber to the required temperature at a rate of 2 ℃/min.

Dielectric constant ε_r was calculated from the measured capacitance C using the following equation:

$$\varepsilon_r = \frac{Cd}{\varepsilon_0 A} \tag{1}$$

where C is the capacitance in farad; ε_0 is the permittivity of free space (8.854×10^{-12} F/m); d is the thickness (m); and A is the area of the samples (m^2). The dielectric constant and dissipation factor were plotted as a function of temperature at a few selected frequencies.

3 Results and discussion

3.1 XRD analysis

XRD patterns of BST borosilicate glass ceramic samples BT5K1L0.0T850, BT5K1L0.0S850, BST5K1L0.4T850 and BST5K1L0.4S850 are shown in Figs. 1–4. XRD pattern of sintered glass ceramic sample BT5K1L0.0T850 shows major crystalline phase of $BaTiO_3$ (BT, JCPDS Card No. 34-0129) and secondary phase of $Ba_2TiSi_2O_8$ (BTS, JCPDS Card No. 22-0513) (Fig. 1) [19–22]. Figure 2 depicts the XRD pattern of glass ceramic sample BT5K1L0.0S850. This pattern is found to be similar as BT5K1L0.0T850, only has a little difference in low intensity peaks of secondary phase. The comparative studies of these XRD patterns for 3 h and 6 h show that 6 h sintering time gives better crystallization. In glass ceramic

Table 1 Sample code, density, crystallite size, breaking strength, elastic modulus, strain and toughness of glass ceramic samples

Glass ceramic sample code	Density (g/cm^3)		Crystallite size (nm)		Breaking strength (MPa)	Elastic modulus (GPa)	Strain	Toughness (MJ/m^3)
	Green pellets	Sintered pellets	L_{DS}	L_{WH}				
BT5K1L0.0T850	3.07	3.36	46.34	54.03	757.85	3.041±0.001	2.39×10^{-3}	131
BT5K1L0.0S850	3.07	3.38	44.43	50.56	2204.15	5.664±0.012	2.64×10^{-3}	614
BST5K1L0.4T850	2.95	3.13	35.62	42.89	4849.44	5.587±0.001	2.00×10^{-3}	3142
BST5K1L0.4S850	2.95	3.22	27.99	40.95	11294.49	7.070±0.001	2.80×10^{-3}	11824

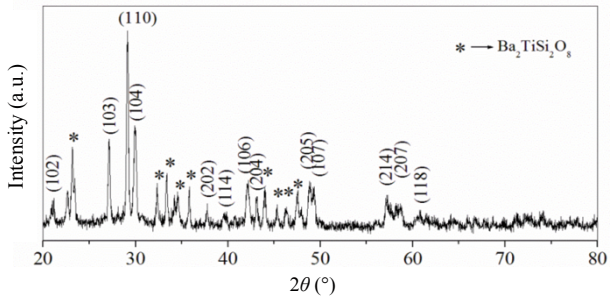

Fig. 1 XRD pattern of glass ceramic sample BT5K1L0.0T850.

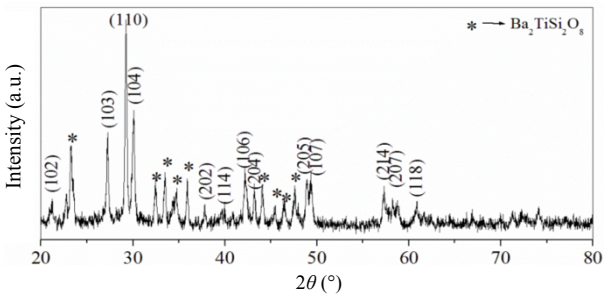

Fig. 2 XRD pattern of glass ceramic sample BT5K1L0.0S850.

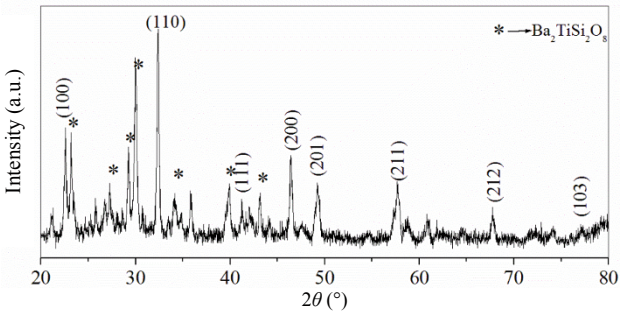

Fig. 3 XRD pattern of glass ceramic sample BST5K1L0.4T850.

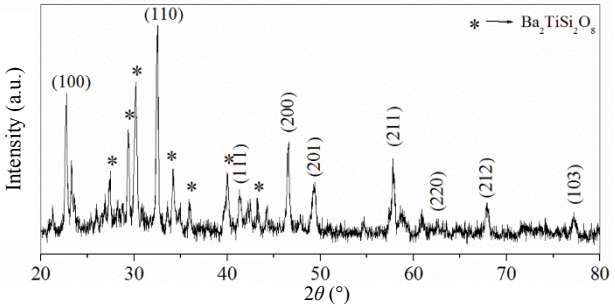

Fig. 4 XRD pattern of glass ceramic sample BST5K1L0.4S850.

samples BT5K1L0.0T850 and BT5K1L0.0S850, there is slight shifting of high intensity peak near 29.5° to a smaller angle due to the tetragonal distortion or crystal clamping. The crystal structure of BT is hexagonal. The lattice parameters for glass ceramic sample BT5K1L0.0T850 are $a = 5.75$ Å, $b = 13.87$ Å and $c = 2.38$ Å. XRD pattern of glass ceramic sample BST5K1L0.4T850 ($x = 0.4$) is shown in Fig. 3, and it confirms the formation of major crystalline phase of BST along with secondary phase of BTS which is similar to XRD pattern of glass ceramic sample BST5K1L0.4S850 sintered for 6 h (Fig. 4) [23]. The crystallite size decreases with increasing the sintering time for the crystallization of the calcined glass samples.

WH plots for all glass ceramic samples are shown in Figs. 5–8. The particle size and strain are obtained by comparing the trend line equation from WH plots and listed in Table 1. The particle sizes obtained from both methods (Debye–Scherer formula and WH plots) show quite different values for corresponding samples. This difference in particle size obtained from two methods occurs due to strain broadening in the samples. The strain for glass ceramic sample BT5K1L0.0T850 is observed to be 2.39×10^{-3}, while it is 2.64×10^{-3} for glass ceramic sample BT5K1L0.0S850. Thus, the strain broadening between the particles increases with sintering time which is clear from Table 1. The positive value of strain between the particles shows the tensile strain in BST glass ceramics.

3.2 Microstructural analysis

SEM micrographs of BST borosilicate glass ceramic samples BT5K1L0.0T850, BT5K1L0.0S850, BST5K1L0.4T850 and BST5K1L0.4S850 are shown in Figs. 9–12. Figure 9 shows the SEM image of glass ceramic sample BT5K1L0.0T850. The interconnected grains with non uniform grain distribution of the major phase of BST inside the glassy matrix are observed. Figure 10 depicts the micrograph of glass ceramic sample BT5K1L0.0S850, and it shows the dense microstructure of grains of smaller size and this confirms nucleation of crystallites in glassy network. Well developed and interconnected grain crystallite phase in the glass matrix of BST is found in SEM image of glass ceramic sample BST5K1L0.4T850 as shown in Fig. 11. The better nucleation is seen in the glass ceramic sample due to heat treatment of 6 h instead of 3 h (Fig. 12). Finally, these micrographs show almost the same grain geometry, only with the difference observed in the densification of the phase formation of crystalline phase. The grain size and porosity in glassy matrix depend upon the sintering as well as glass composition. The grain size is decreased

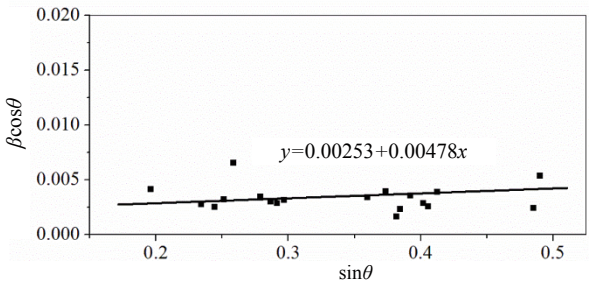

Fig. 5 WH plot of glass ceramic sample BT5K1L0.0T850.

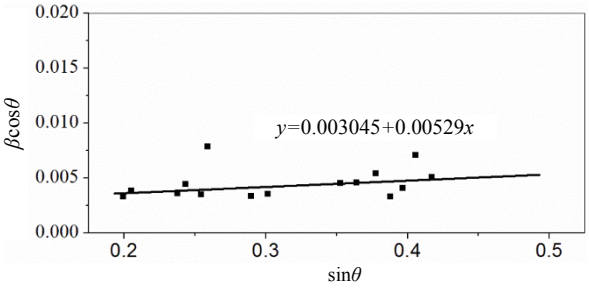

Fig. 6 WH plot of glass ceramic sample BT5K1L0.0S850.

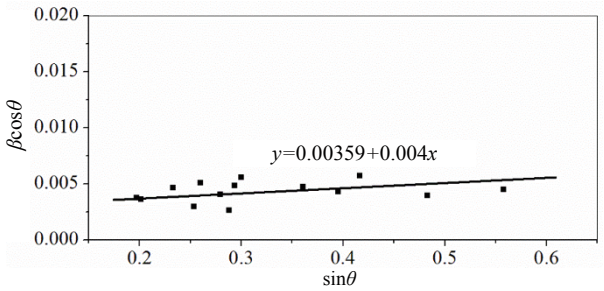

Fig. 7 WH plot of glass ceramic sample BST5K1L0.4T850.

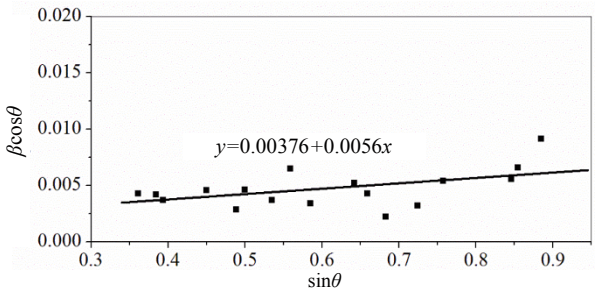

Fig. 8 WH plot of glass ceramic sample BST5K1L0.4S850.

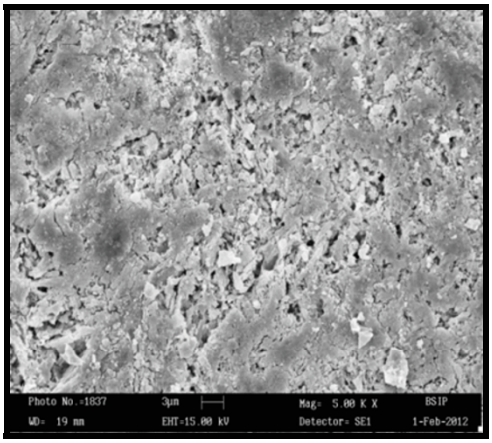

Fig. 9 SEM micrograph of glass ceramic sample BT5K1L0.0T850.

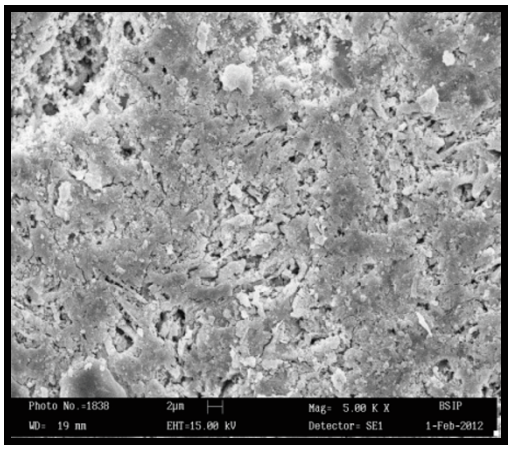

Fig. 10 SEM micrograph of glass ceramic sample BT5K1L0.0S850.

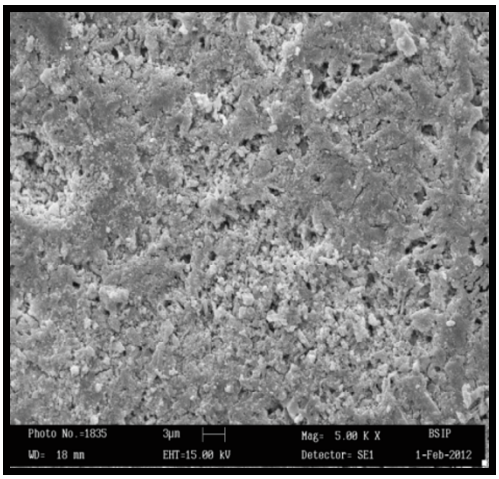

Fig. 11 SEM micrograph of glass ceramic sample BST5K1L0.4T850.

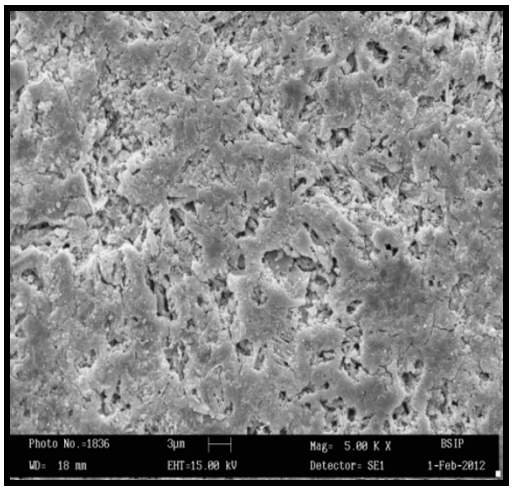

Fig. 12 SEM micrograph of glass ceramic sample BST5K1L0.4S850.

with increase of sintering time and increase of the content of SrO in the glass ceramic samples [5].

3.3 Density measurements

The geometrical densities of green and sintered pellets of samples BT5K1L0.0T850, BT5K1L0.0S850, BST5K1L0.4T850 and BST5K1L0.4S850 have been listed in Table 1. The density of green pellets of samples BT5K1L0.0 is found to be 3.07 g/cm^3, and that of sintered pellets of sample BT5K1L0.0T850 is 3.36 g/cm^3 while for BT5K1L0.0S850 is 3.38 g/cm^3. The density of sintered glass ceramic samples is found to be higher than the reported value of density of glass ceramic samples formed by controlled crystallization of glass for the same system [24]. This shows that densification of glass ceramic samples on sintering increases with increasing the sintering time. This is also confirmed by XRD and SEM analyses. Similarly, the densities of glass ceramic samples BST5K1L0.4T850 and BST5K1L0.4S850 also increase with sintering time. Not only the sintering effect on density but the compositional effects are observed in these glass ceramic samples. With addition of Sr content, the density of glass ceramic samples decreases due to less density of Sr (2.6 g/cm^3) than Ba (3.5 g/cm^3).

3.4 Mechanical behavior

Mechanical properties depend upon crystallize size and porosity, and all such parameters depend on soaking time of sintering as well as compositions of the glass ceramics. Stress vs. strain measurements were carried out in compressive mode of uniform cylindrical glass ceramic samples BT5K1L0.0T850, BT5K1L0.0S850, BST5K1L0.4T850 and BST5K1L0.4S850 as shown in Figs. 13 and 14. The compressive study of glass ceramic sample BT5K1L0.0T850 reveals that Hooke's law of elasticity follows up to load of 757.85 MPa (Fig. 13(a)). Figure 13(b) shows the variation of strain with compressive stress and it varies directly up to load 2204.15 MPa. The glass ceramic sample BT5K1L0.0S850 withstands more loads as compared to glass ceramic sample BT5K1L0.0T850. Mechanical strength of glass ceramic samples increases with decreasing grain size or crystallite size, as clear from Table 1 [5]. Thus, compressive mechanical strength increases with increasing the sintering time for crystallization. This high elastic modulus may be attributed to van der Waals–London attractive

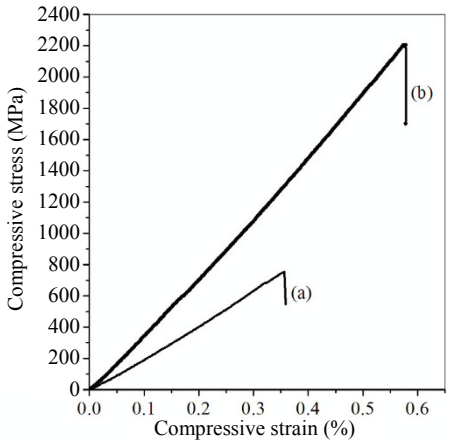

Fig. 13 Variations of compressive strain vs. compressive stress: (a) BT5K1L0.0T850 and (b) BT5K1L0.0S850.

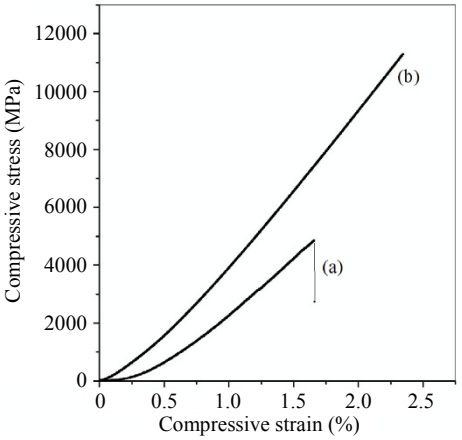

Fig. 14 Variations of compressive strain vs. compressive stress: (a) BST5K1L0.4T850 and (b) BST5K1L0.4S850.

interactions and it varies inversely with size of particles. Elastic modulus is determined by slope of stress–strain curve at any point in linear portion of the curve. The value of elastic modulus is found to be 5.664±0.012 GPa for BT5K1L0.0S850, while it is 3.041±0.001 GPa for BT5K1L0.0T850. Elastic property of glass ceramic sample BST5K1L0.4T850 describes that the Hooke's law does not be obeyed initially, and it shows the ductile nature which is due to 40% addition of Sr content in glass ceramic sample BST5K1L0.4T850. Compressive stress follows linearly with further increase of load up to yield point 4849.44 MPa (Fig. 14(a)). Thus, addition of Sr content increases the mechanical strength of glass ceramic sample. Figure 14(b) shows that ductileness of glass ceramic sample BST5K1L0.4S850 decreases with increasing sintering time for crystallization. The

compressive strength is found to be 11 294.49 MPa. This high value of strength is due to addition of Sr content as well as soaking time for sintering. The glass ceramic sample BST5K1L0.4S850 is found more elastic than others and its elastic modulus is 7.070±0.001 GPa. This value of elastic modulus is much higher than those of other reported glass ceramics [25–27]. The compressive strength, elastic modulus and toughness of these glass ceramic samples have been listed in Table 1.

The toughness of glass ceramic sample BT5K1L0.0T850 is found to be 131 MJ/m^3, whereas its value for glass ceramic sample BT5K1L0.0S850 is 614 MJ/m^3. Thus, with increasing the soaking time of sintering, the ability to resist the crack in glass ceramic sample increases, and it confirms the sintering time dependence on densification. Dependence of densification is also observed from SEM micrographs and XRD analysis. When 40 mol% of Sr content is added in the glass ceramic system of BST borosilicate, then toughness is increased up to value of 3142 MJ/m^3 for glass ceramic sample BST5K1L0.4T850 and 11 824 MJ/m^3 for sample BST5K1L0.4S850. Such type of glass ceramics can be used for high load bearing applications. These glass ceramics are having high resistance to corrosion and also withstand high temperature.

3.5 Dielectric behavior

The dielectric behavior of glass ceramic samples depends on various factors such as the nature and amount of crystallinity of crystalline phases, crystallite size, grain size and grain boundary morphology, pyrochlore phases, crystal clamping and the connectivity of the high permittivity perovskite crystals in the low permittivity glassy matrix. The nature of crystalline phases and microstructure of glass ceramics can be controlled by heat treatment conditions during the crystallization of glass to glass ceramics. The solid solution of barium titanate and strontium titanate ceramic to form $(Ba_{1-x}Sr_x)TiO_3$ have significant importance for technological point of view, as such glass ceramics have very high dielectric constant. The ferroelectric phase transition in these glass ceramics has been controlled by composition as well as heat treatment schedule.

Figures 15 and 16 depict the variations of dielectric constant and dielectric loss with temperature for glass ceramic samples BT5K1L0.0T850 and BST5K1L0.4T850 at frequencies 20 Hz, 100 Hz, 1 kHz, 10 kHz and 100 kHz. The dielectric behavior of glass ceramic sample BT5K1L0.0T850, sintered for 3 h at 850 ℃, is shown in Fig. 15. The double phase transition is observed at temperatures of 60 ℃ and 125 ℃, and it is similar to previously reported results on $(BaSr)TiO_3$ by Zhang *et al*. [28]. The double anomaly occurs due to successive transitions from orthorhombic to tetragonal and tetragonal to cubic crystal structures. The ferroelectric features are confirmed by symmetry breaking in dielectric constant. Here, the second phase transition is also attributed to the transition of ferroelectric phase to paraelectric at Curie temperature of 125 ℃. The highest value of dielectric constant is found to be 31 497 at frequency of 20 Hz. The dielectric loss at low frequencies increases gradually with increasing the temperature, and its value on room temperature at 20 Hz is found to be 0.01. The peak position variation with temperature is non-monotonic. This may be due to non uniform distribution of secondary phase formation in glassy matrix or defects produced by crystal clamping. Figure 16 shows the dielectric behavior of glass ceramic sample BST5K1L0.4T850 which is derived by 60/40 (in mol%) of Ba/Sr ratio for the same glass system, and it is sintered for 3 h. The dielectric constant for this glass ceramic sample at 20 Hz is observed to be 32 349. This value of dielectric constant is greater than the value of dielectric constant at the same frequency for Sr free glass ceramic sample BT5K1L0.0T850. This increase in the value of dielectric constant is attributed to the higher conductivity difference among the crystalline phase, pyrochlore phase and glass interface. The dielectric loss increases gradually with increasing the temperatures for frequencies of 20 Hz, 10 kHz and 100 kHz, and its value for 20 Hz at room temperature is 0.01.

The variations of dielectric constant and dielectric loss with temperature at above mentioned frequencies for glass ceramic samples BT5K1L0.0S850 and BST5K1L0.4S850 are shown in Figs. 17 and 18, which are derived by sintering of 6 h soaking time. The sintering time for the crystallization affects the value of dielectric constant but it does not change the dielectric behavior of the glass ceramic samples. Curie temperature of 6 h sintered glass ceramics is decreased, and this may lead to reduction of residual glass and pyrochlore phases in the glassy matrix. Figure 17 depicts the dielectric behavior of glass ceramic sample

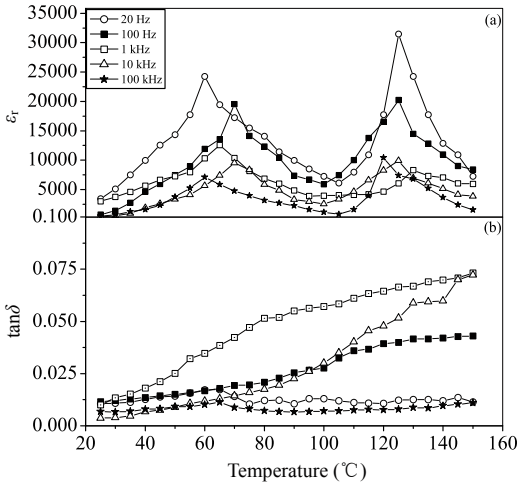

Fig. 15 Variations of (a) dielectric constant ε_r and (b) dissipation factor tanδ with temperature at different frequencies for glass ceramic sample BT5K1L0.0T850.

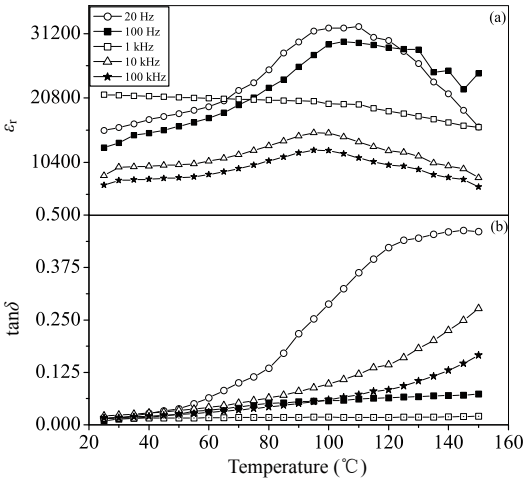

Fig. 16 Variations of (a) dielectric constant ε_r and (b) dissipation factor tanδ with temperature at different frequencies for glass ceramic sample BST5K1L0.4T850.

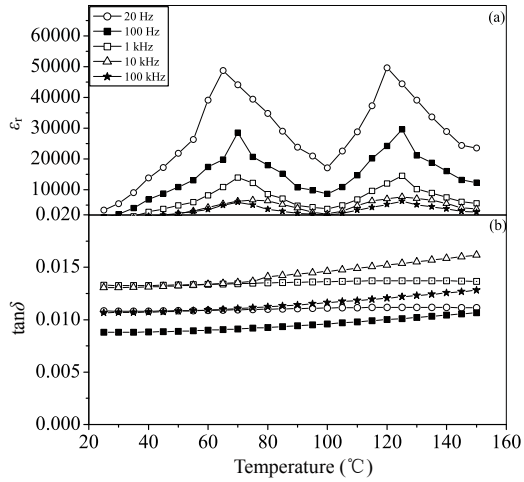

Fig. 17 Variations of (a) dielectric constant ε_r and (b) dissipation factor tanδ with temperature at different frequencies for glass ceramic sample BT5K1L0.0S850.

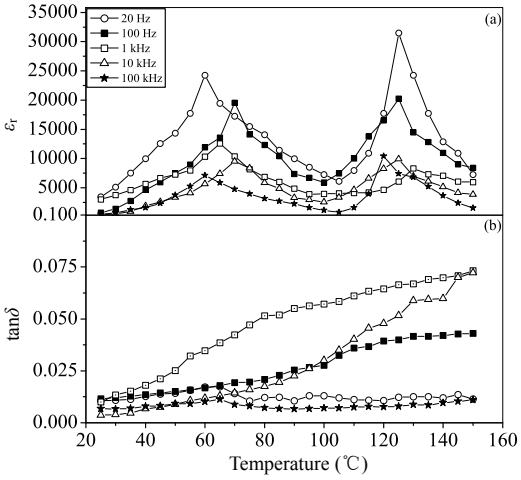

Fig. 18 Variations of (a) dielectric constant ε_r and (b) dissipation factor tanδ with temperature at different frequencies for glass ceramic sample BST5K1L0.4S850.

BT5K1L0.0S850, and this pattern shows that the dielectric constant is increased up to 49 612 from 31 497 with increase in sintering time. This high value of dielectric constant is attributed to interfacial or space charge polarization which is arising from the conductivity difference among the various phases such as major BT/BST phase, secondary phase and glass matrix interface [29]. In 6 h sintered glass ceramic samples, the amount of secondary phase is less as compared to that of 3 h, and hence, there is large conductivity difference between semiconducting grains and insulating glassy matrix. Curie temperature for glass ceramic sample BT5K1L0.0S850 is found to be 120 ℃. The dielectric loss for this glass ceramic sample is almost independent of temperature which is good indication for high energy storage device applications such as capacitors and barrier layer capacitors. The value of dielectric loss for 20 Hz frequency at room temperature is 0.01. The variation of dielectric constant and dielectric loss with temperature at frequencies 20 Hz, 100 Hz, 1 kHz, 10 kHz and 100 kHz of glass ceramic sample BST5K1L0.4S850 is shown in Fig. 18. The peak value of dielectric constant is observed at 20 Hz and it is found to be 39 532. The

dielectric loss for glass ceramic samples is not much influenced by the temperature variations, and its value at room temperature corresponding to 20 Hz is found to be 0.01. The values of dielectric constant and dielectric loss at various frequencies have been listed in Table 2. These glass ceramic samples show the ferroelectric behavior due to addition of La_2O_3. The solid solution crystallites of BT/BST become semiconducting due to diffusion of La ions in the solution. Strontium titanate leads to the formation of electronic defects/vacancies of titanium cation with addition of La_2O_3 and depends on the doping level and processing condition as per the following equations, where all symbols are in Kröger–Vink notations.

$$La_2O_3 + 2TiO_2 \xrightarrow{SrTiO_3} 2La_{Sr}^{\bullet} + 2Ti_{Ti}^{\times} + 6O_O + \frac{1}{2}O_2 + 2e' \quad (2)$$

$$2La_2O_3 + 3TiO_2 \xrightarrow{SrTiO_3} 4La_{Sr}^{\bullet} + 3Ti_{Ti}^{\times} + V_{Ti}'''' + 12O_O \quad (3)$$

The doping of La_2O_3 in small concentration in perovskite ceramics induces n-type semiconductivity by electronic compensation which is given by Eq. (4), but higher concentration of La^{3+} creates titanium vacancies given by Eq. (5).

$$La^{3+} \xrightarrow{SrTiO_3} La_{Sr}^{\bullet} + 3e' \quad (4)$$

$$La^{3+} \xrightarrow{SrTiO_3} La_{Sr}^{\bullet} + \frac{1}{4}V_{Ti}'''' \quad (5)$$

4 Conclusions

Bulk transparent BST borosilicate glasses were prepared successfully by melt quench method, and their glass ceramics were formed by solid state sintering route. XRD patterns of these glass ceramic samples confirm the formation of the major perovskite phase of $BaTiO_3$ /(Ba,Sr)TiO_3 along with trace amount of secondary phase of $Ba_2TiSi_2O_8$. The crystallite size decreases with increasing the sintering time or increasing the content of SrO. The mechanical strength of glass ceramic samples increases with decreasing the crystallite size. The value of dielectric constant is found to maximum (49 612) for glass ceramic sample BT5K1L0.0S850. The dielectric constant is increased with increasing the soaking time for sintering of glass ceramics. These glass ceramic samples show the ferroelectric behavior in barium rich glass ceramic samples.

Acknowledgements

The authors gratefully acknowledge the University Grant Commission (UGC), New Delhi, India for financial support under major research project F.No.37-439/2009 (SR).

References

[1] Beall GH, Pinckney LR. Nanophase glass-ceramics. *J Am Ceram Soc* 1999, **82**: 5–16.

[2] Thakur OP, Kumar D, Parkash O, *et al*. Electrical characterization of strontium titanate borosilicate glass ceramics system with bismuth oxide addition using impedance spectroscopy. *Mater Chem Phys* 2003, **78**: 751–759.

[3] Henry J, Hill RG. The influence of lithia content on the properties of fluorphlogopite glass-ceramics. II. Microstructure hardness and machinability. *J Non-Cryst Solids* 2003, **319**: 13–30.

[4] Schneider SJ. *Engineered Materials Handbook Volume 4*: *Ceramics and Glasses*. Materials Park, Ohio: ASM International, 1991.

[5] Gomaa MM, Abo-Mosallam HA, Darwish H. Electrical and mechanical properties of alkali barium

Table 2 Dielectric characteristics of glass ceramic samples BT5K1L0.0T850, BT5K1L0.0S850, BST5K1L0.4T850 and BST5K1L0.4S850

Glass ceramic sample code	Curie temperature T_C (℃)	Room temperature dielectric parameters at 20 Hz		Value of maximum dielectric constant ε_r				
		ε_r	tanδ	20 Hz	100 Hz	1 kHz	10 kHz	100 kHz
BT5K1L0.0T850	125	3448	0.01	31497	20712	9897	8366	10420
BT5K1L0.0S850	120	3370	0.01	49612	29956	14707	8142	6267
BST5K1L0.4T850	110	15695	0.01	32349	30032	21441	15195	12276
BST5K1L0.4S850	100	20758	0.01	39532	32310	22177	18365	23447

titanium alumino borosilicate glass-ceramics containing strontium or magnesium. *J Mater Sci*: *Mater El* 2009, **20**: 507–516.

[6] Haung Q, Gao L, Sun J. Effect of adding carbon nanotubes on microstructure, phase transformation, and mechanical property of $BaTiO_3$ ceramics. *J Am Ceram Soc* 2005, **88**: 3515–3318.

[7] Jana F, Shirane J. *Ferroelecrtrics Crystals*. Oxford: Peragamon Press, 1962.

[8] Divya PV, Kumar V. Crystallization studies and properties of $(Ba_{1-x}Sr_x)TiO_3$ in borosilicate glass. *J Am Ceram Soc* 2007, **90**: 472–476.

[9] Divya PV, Vignesh G, Kumar V. Crystallization studies and dielectric properties of $(Ba_{0.7}Sr_{0.3})TiO_3$ in bariumaluminosilicate glass. *J Phys D*: *Appl Phys* 2007, **40**: 7804–7810.

[10] Gorzkowski EP, Pan M-J, Bender B. Glass-ceramics of barium strontium titanate for high energy density capacitors. *J Electroceram* 2007, **18**: 269–276.

[11] Gorzkowski EP, Pan M-J, Bender BA, *et al*. Effect of additives on the crystallization kinetics of barium strontium titanate glass–ceramics. *J Am Ceram Soc* 2008, **91**: 1065–1069.

[12] Zhang Q, Wang L, Luo J, *et al*. Improved energy storage density in barium strontium titanate by addition of $BaO–SiO_2–B_2O_3$ glass. *J Am Ceram Soc* 2009, **92**: 1871–1873.

[13] Isaka N, Ohkawa K, Kiyono H, *et al*. Effects of glass components on crystallization and dielectric properties of BST glass–ceramics. *J Mater Sci*: *Mater El* 2008, **19**: 1233–1239.

[14] Rangarajan B, Jones B, Shrout T, *et al*. Barium/lead-rich high permittivity glass–ceramics for capacitor applications. *J Am Ceram Soc* 2007, **90**: 784–788.

[15] Chen G, Zhang W, Liu X, *et al*. Preparation and properties of strontium barium niobate based glass-ceramics for energy storage capacitors. *J Electroceram* 2011, **27**: 78–82.

[16] Song J, Chen G, Yuan C, *et al*. Effect of the Sr/Ba ratio on the microstructures and dielectric properties of $SrO–BaO–Nb_2O_5–B_2O_3$ glass–ceramics. *Mater Lett* 2014, **117**: 7–9.

[17] Yadav AK, Gautam C, Singh P. Crystallization kinematics and dielectric behavior of $(Ba,Sr)TiO_3$ borosilicate glass ceramics. *New Journal of Glass and Ceramics* 2012, **2**: 126–131.

[18] Yadav AK, Gautam CR. A review on crystallisation behaviour of perovskite glass ceramics. *Adv Appl Ceram* 2014, **113**: 193–207.

[19] Gautam CR, Yadav AK, Singh P. Synthesis, crystallisation and microstructural study of perovskite $(Ba,Sr)TiO_3$ borosilicate glass ceramic doped with La_2O_3. *Mater Res Innov* 2013, **17**: 148–153.

[20] Arend H, Kihlborg L. Phase composition of reduced and reoxidized barium titanate. *J Am Ceram Soc* 1969, **52**: 63–65.

[21] Alfors JT, Stinson MC, Matthew RA, *et al*. Seven new barium minerals from eastern Fresno County, California. *Am Mineral* 1965, **50**: 314–340.

[22] Yadav AK, Gautam CR, Gautam A, *et al*. Structural and crystallization behavior of $(Ba,Sr)TiO_3$ borosilicate glasses. *Phase Transitions* 2013, **86**: 1000–1016.

[23] Joseph J, Vimala TM, Raja J, *et al*. Structural investigations on the $(Ba,Sr)(Zr,Ti)O_3$ system. *J Phys D*: *Appl Phys* 1999, **32**: 1049–1054.

[24] Gautam C, Yadav AK, Mishra VK, *et al*. Synthesis, IR and Raman spectroscopic studies of $(Ba,Sr)TiO_3$ borosilicate glasses with addition of La_2O_3. *Open Journal of Inorganic Non-metallic Material* 2012, **2**: 47–54.

[25] Dupen B. Measuring Young's modulus with metal flatstock. *The Technology Interface Journal* 2007, available at http://technologyinterface.nmsu.edu/Fall07/10_Dupen/index.pdf.

[26] Ryu S-S, Kim H-T, Kim H-J, *et al*. Characterization of mechanical properties of $BaTiO_3$ ceramic with different types of sintering aid by nanoindentation. *J Ceram Soc Jpn* 2009, **117**: 811–814.

[27] Yadav AK. Synthesis, microstructure and dielectric properties of barium strontium titanate borosilicate glass ceramics. PhD Thesis. Lucknow, India: University of Lucknow, 2013: 294–312.

[28] Zhang Y, Ma T, Wang X, *et al*. Two dielectric relaxation mechanisms observed in lanthanum doped barium strontium titanate glass ceramics. *J Appl Phys* 2011, **109**: 084115.

[29] Thakur OP, Kumar D, Parkash O, *et al*. Crystallization, microstructure development and dielectric behaviour of glass ceramics in the system $[SrO·TiO_2]–[2SiO_2·B_2O_3]–La_2O_3$. *J Mater Sci* 2002, **37**: 2597–2606.